Title: Fabrication of ZnO nanorods by atmospheric pressure solid source CVD using ethanol-assisted low temperature vaporization

Sawako Miyamoto[1,2], Tetsuya Hasegawa[1], Hiroyuki Takahashi[3], Tetsu Yonezawa[3], Hajime Kiyono[2], Takashi Yanase[4], Taro Nagahama[2] and Toshihiro Shimada[2]

[1] Department of Chemistry, The University of Tokyo, Bunkyo-ku 113-0033, Japan

[2] Division of Materials Chemistry, Faculty of Engineering, Hokkaido University, Sapporo, Hokkaido 060-8628, Japan

[3] Division of Materials Science and Engineering, Faculty of Engineering, Hokkaido University, Sapporo, Hokkaido 060-8628, Japan

[4] Frontier Chemistry Center, Faculty of Engineering, Hokkaido University, Sapporo, Hokkaido 060-8628, Japan

Received: ; E-mail: shimadat@eng.hokudai.ac.jp

We report a method to produce vapor species from ZnO powder for the fabrication of ZnO nanorods. Mixing ethanol vapor with the inert carrier gas substantially lowered the gasification temperature of ZnO. c-axis aligned ZnO nanorods were obtained by dispersing gold nanoparticles on Si substrates. The growth was identified as a vapor-solid (VS) mechanism. Choice of the substrate materials and their surface morphology were both critically important to control the shapes and orientation of grown ZnO.

1. Introduction

ZnO nanorods (NRs) have potential application in solar cells[1,2], chemical[3] and ultraviolet[4] sensors and piezoelectronic devices[5] in small scales. There have been many reports regarding methods to fabricate ZnO NRs and devices using them. They are classified in two categories, vapor phase process[6] and solution process[7,8]. Vapor phase process has a potential advantage of crystal quality[9] and easy doping without contamination[10]. Popular vapor-phase methods include chemical vapor deposition (CVD)[11] and thermal evaporation. Widely used CVD uses harmful materials which require rigorous control of exhaust gas systems in general. Thermal evaporation of ZnO has also problems because the control of vapor pressure of Zn is difficult in oxidative atmospheres[12] and evaporation of ZnO itself requires high temperatures over 1000 ^{o}C[13]. Using reducing reagents such as carbon is essential to decrease the gasification temperature of ZnO but it is still as high as 900 ^{o}C[14]. In this work, we attempted to lower the gasification temperature of ZnO by solid-gas reaction with chemical vapors. Evaporation kinetics were studied by thermogravimetric analysis (TGA). ZnO with various morphologies was obtained by changing the substrate materials including those with gold nanoparticle (NP) catalyst.

2. Experimental

First, the ZnO gasification under chemical vapor flow was studied by TGA using a Cahn C-2000 electric microbalance (Fig.1 (a)). About 15mg of ZnO powder was put on an alumina sample holder. The temperature was raised at a rate of 10^{o}C/min to the final temperature set at 700^{o}C, 750^{o}C, 800^{o}C, 850^{o}C, and 900^{o}C, which were kept for a certain time. Argon gas (99.99% purity) bubbled through a liquid (ethanol, water or acetone) was introduced directly to the quartz tube with the flow rate of 96 sccm. We conducted a control experiment in which argon gas was flown without chemical vapors while keeping other conditions equivalent.

Second, we examined the possibility of using the ethanol vapor-assisted process to fabricate ZnO NRs. We built a cold-wall type CVD chamber illustrated in Fig.1(b). Substrates and source materials were controlled by Joule heating of silicon plates. Temperatures during the growth were

measured by radiation thermometer. ZnO powder (99.9%, Kojundo Chemical Lab.) was used as source material. We attempted the growth of ZnO on ITO coated glass substrates, Si (100) substrates, and Si (100) dispersed with gold NPs. SiO_2 layer on the surface of Si substrate was removed by 5% HF solution just prior to the ZnO growth experiments. Si (100) with gold NPs was prepared by drop-casting a solution containing gold NPs and annealing it at 300 ^oC for 30 min in air. Gold NPs were prepared by reducing $HAuCl_4$ by sodium citrate[15] and their diameter was 16.5 ±1.3 nm. The substrate temperatures were varied between 300 and 700 ^oC during the growth. 1 atm argon gas was used as a carrier gas in the quartz tube. Argon gas (99.99%) flowed through an ethanol bubbler was kept at room temperature before being introduced to the quartz tube. Exhaust gas was analyzed by infrared spectroscopy using an Si window (SHIMADZU FTIR-8400). The grown ZnO was evaluated by scanning electron microscopy (SEM; JEOL JSM-6300F), x-ray diffraction (XRD; Rigaku SA-HF3) and x-ray photoelectron spectroscopy (XPS; JEOL JPS-9200), in terms of surface morphology, crystallinity and orientation and chemical composition, respectively.

3. Results and Discussion

3.1.TGA

We measured the weight change of ZnO in a furnace heated under a gas flow after bubbling various liquids. When water or acetone was in the bubbler, no detectable weight change was observed at 700 ^oC. However, when ethanol was used, weight loss was observed above 700 ^oC and above. Figure 2 shows two typical TGA results with the final temperature of 700 ^oC with and without ethanol bubbling. Apparent weight gains around 8 x 10^3 s are due to the instrumental error caused by convection of the carrier gas. The TGA curve with ethanol bubbling shows that ZnO powder was gasified at 700 ^oC. This temperature is substantially lower than those in previous reports. Total weight loss was about 72% after TG curve became flat (6 x 10^4 s). ZnO was not totally gasified and black solid remained. When the ethanol vapor was not introduced, there was no net weight loss from start to end.

We calculated the rate constants k of weight loss at various temperatures from the slope of TGA with ethanol vapor and plotted it in an Arrhenius plot in Fig. 3. Activation energy of gasification reaction between ZnO and ethanol vapor was estimated to be 83.7 $\pm$ 3.7 kJ/mol from the plot. Residual solid on the sample holder was examined by XRD and Raman spectroscopy. It was identified as a mixture of ZnO and amorphous carbon when the gasification temperature was between 700 and 850 ^{o}C. Probably amorphous carbon started to cover ZnO during the reaction and further gasification was hindered at 80% weight loss. Indeed, a broad peak at 2θ = 25.52^{o} appeared from the sample kept at 900 ^{o}C, which corresponds to the XRD of amorphous carbon. In this case the weight loss was 90.5 %, which was larger than those in other conditions. In conclusion, TGA revealed that ZnO reacted with ethanol vapor above 700^{o}C and was gasified. We therefore used ethanol as the gasification reagent in the following.

3.2. IR monitoring of the exhaust gas

The exhaust gas tube from the growth chamber was connected to a laboratory built FTIR gas spectrometer[16] in order to study the reaction between ZnO powder and ethanol from the gas product (fig.1 (b)). Figure 4 shows the results of IR before (a) and during (b) the heating of the ZnO source. Absorbance peaks corresponding to ethanol[17] were detected in (a), whereas they became weaker in (b). C=O stretching peaks appeared near 1730cm^{-1} and 2100cm^{-1}, and geminal peaks near 2360cm^{-1} was characteristic to CO_2 gas. From these results, it was confirmed that ethanol was oxidized, not only producing ethylene and hydrogen[18]. The oxidization of ethanol suggests that ZnO is reduced, which is consistent with the gasification of ZnO at low temperature (700 ^{o}C). Although vapor phase species of Zn was not identified from the IR analysis of exhaust gas, it is supposed that some organometallic species of Zn or Zn itself were formed by the reduction. A tentative reaction formula can be summarized as follows, although some organic compound (C, H, O) might be present, depending upon the temperature:

$$CH_3CH_2OH + 4\,ZnO \rightarrow 4\,Zn \uparrow + C + CO_2 + 3H_2O.$$

In the following we observed the deposition of ZnO nanowires on substrates with catalytic activities. Based on the TGA and FTIR results, we believe the deposition mechanism is basically kinematic. Since the vapor pressure of Zn is ~ 1 torr at 400 ^{o}C [19] but that of ZnO is immeasurably small, ZnO is the least volatile species at the substrate temperatures for the growth (400 ^{o}C ~ 650 ^{o}C). Therefore once ZnO is formed, it becomes the only species deposited on the substrate surface. Oxygen might come from the residual CH_3CH_2OH flowing with the carrier gas, or might come from the organometallic Zn formed by the reaction with CH_3CH_2OH. The deposition will compete with the etching by reduction of defective as-deposited ZnO and it probably leads to the characteristic morphology

3.3. Morphology and crystal orientation of grown ZnO

Gray or white films were formed on the substrates (ITO, Si, Au NP-coated Si). The grown material was ZnO on all of the substrates as measured by XRD, but morphology and the crystal orientation were strongly dependent on the substrate materials and the growth temperature. We will first describe the SEM and XRD results to compare the morphology and crystallinity.

Figure 5 shows SEM images of ZnO with nano-scale structures grown on ITO substrates. Figures 5 (a)-(e) show the results of substrate temperature of 400^{o}C, 450^{o}C, 500^{o}C, 550^{o}C, and 600^{o}C, respectively, in the same scale. Branching of NRs was frequently observed below 450 ^{o}C, and small particles are formed at 500 ^{o}C. At higher temperatures (550 ^{o}C and 600 ^{o}C), very long (>20μm) straight thin NRs were formed. XRD of the ZnO grown on ITO shows comparable intensity of (100), (002) and (101) peaks, which is consistent with the randomly oriented NRs in SEM images. The ITO surface was observed by AFM after heating in ethanol/Ar flow at 550^{o}C in order to see the mechanism of random orientation. It was found that root-mean-square roughness of ITO surface was 2 - 3 nm. XRD (not shown) showed randomly oriented ITO crystals (ITO(222) at 2θ = 30.16^{o}, ITO(400) at 2θ = 35.14^{o}). It is reasonable to consider that this roughness and randomness cause the randomly oriented nucleation of ZnO NRs.

The same procedure was used to grow ZnO on Si (100) substrates. Substrate temperature was changed from 300^{o}C to 600^{o}C with 50^{o}C steps. When substrate temperature was higher than or equal to 550^{o}C, nothing was formed on the substrate. Figure 7 shows the SEM images of ZnO grown on Si substrates at 300 ^{o}C - 500 ^{o}C. Films were composed of flakes and their sizes become larger at higher substrate temperatures. When the substrate temperature was 500^{o}C, a hexagonal column was formed as shown in Fig. 7(e), which is the favorite form of ZnO. It should be noted that orientation ratio greatly depends on substrate temperature as shown in Table 1. This suggests that the migration and decomposition of vapor-species occur on the substrate and their rates depend differently on substrate temperature. (002) orientation is preferred when substrate temperature was 450 ^{o}C. Although (002) was also preferred at 350 ^{o}C, the crystallinity was poorer than 450 ^{o}C. The mechanism of the orientation at particular temperature range is not clear at this present, but it is suggested that the competition between the growth and etching is sometimes contributes to this kind of phenomenon.

Figure 8 shows ZnO NRs grown on Si(001) substrates dispersed with Au NPs. The reaction time was 30min. Substrate temperature was set at 450 ^{o}C because c-orientation ratio was the highest on Si (100) and amorphous structures were the least on ITO at this temperature. Aligned NRs are observed in Fig. 8. Their diameter and length were 20-30 nm and ~500 nm, respectively. XRD after the growth showed a Au(111) peak (2θ = 38.2^{o}) with substantial intensity. No other peaks corresponding to gold were observed in XRD.

In order to understand the effect of gold NPs, two areas with different Au NP density were prepared on the same Si (100) substrate. Figure 9 shows the SEM images of gold NPs and ZnO NRs grown at the same condition with Fig. 8. It is revealed that the density of gold NPs affects the diameter and density of ZnO NRs greatly. When the density of gold NPs was small, thicker ZnO NRs (diameter: about 100 nm) were grown. However, when the density was large, thinner NRs (diameter: about 15 nm) were grown densely. This result clearly shows the competition among gold NPs for the ZnO nucleation. It suggests that the catalytic activity of gold NPs is essential in

the decomposition process of vapor-species created by the reaction between ZnO and ethanol, or the crystallization process of ZnO.

There are two major crystal growth mechanisms of NRs fabricated by vapor-phase method using catalysts such as gold NPs, namely, vapor-solid (VS) and vapor-liquid-solid (VLS) mechanisms[20,21]. The position of the catalytic NPs in the grown NRs is important to distinguish them. It might move to the growing front of NRs in the case of VLS or it might rest on the bottom of NRs in the case of VS. In order to clarify this, the surface of ZnO NRs was examined by XPS. The sample was ZnO NRs with the length of 500 nm. The result is shown in Fig.10 (a) and (b). There was no Au signal detected on the surface of ZnO. For comparison, Si substrate with gold NPs that was heated at 450 ^{o}C for 30 min without ZnO source heating was measured by XPS. Gold peaks were observed as shown in Fig. 10 (c). It is therefore concluded that gold NPs stayed at the bottom of the ZnO NRs.

The growth mechanism can also be analyzed by measuring the growth speed of ZnO NRs as a function of time. The growth speed was estimated by the lengths of ZnO NRs in SEM images. The results are summarized in Fig. 11, in which significant leveling was observed. This observation can be explained by catalytic gold NPs are concealed as the growth proceeds. Both results indicate that the growth in the present technique follows VS mechanism. It is consistent with the VS growth of ZnO at low temperature (< 850 ^{o}C) without the ethanol vapor[20].

From the results presented above, it can be seen that the morphology and the crystal orientation are strongly dependent on the composition of substrate surfaces. It is due to the difference in the catalytic activity of the surface, which is most clearly evidenced in the case of gold NPs. The growth speed was roughly estimated from the film thickness divided by reaction time, which was in the order that Si (100) with gold NPs > ITO >> Si (100).

Since the alignment of ZnO NRs is important for applications, possible improvement to orient the NRs should be discussed. As shown in Table 2, a portion of (002) orientated NRs is in the order Si (100) >> Si(100) with gold NPs > ITO. This suggests that the roughness of surface affects the orientation, probably through the stability of (001) surface and favored kinetics along c-axis growth of ZnO in addition to epitaxy-like lattice orientation effect[22]. Si (100) surface is the flattest of the

three substrates and ITO surface is rough in nanometer scales (Fig. 6). According to XRD results, gold NPs oriented (111) facet to the surface, which helped orientation of ZnO better than that on ITO. Nevertheless the orientation on gold NPs was not perfect. The surface curvature of gold NPs might affect the orientation, in which surface energy of the facets play an important role[23].

4. Conclusion

We examined a facile method to grow ZnO NRs, which is a cold wall atmospheric CVD using ethanol vapor to assist the gasification of ZnO. It was shown that gasification temperature of ZnO powder was much reduced to 700 ^{o}C by introducing the ethanol vapor. By comparing the results using various substrates, catalytic activity of the surface is essential to the growth of ZnO NRs. ZnO NRs grew in the case of Si(100) dispersed with gold NPs, which is due to gold catalytic activity and its nanoscale size and NRs are oriented to show Au(111) surface under the growth conditions. From XPS and a kinematic analysis, it is concluded that the growth follows a VS mechanism. Not only NRs but also branching nanostructures and nanoflakes could be obtained by changing the substrates.

Acknowledgment: A part of the present work was supported from Tanikawa Fund for Promotion of Thermal Technology. Raman spectroscopy was performed using the facility of CRIS, Hokkaido University.

References

1 K. Nonomura, T.Loewenstein, E.Michaelis, T.Yosjida, H. Minoura, D.Schlettwein, *Phys. Chem. Chem. Phys.* **2006**, 8, 3867-3875.

2 K. Takanezawa, K. Hirota, Q.S. Wei, K. Tajima, K. Hashimoto, *J. Phys. Chem. C* **2007**, 111, 7218 - 7223.

3 P.M. Parthangal, R.E. Cavicchi, M.R. Zachariah, *Nanotechnology* **2006**, 17, 3786-3790.

4 S.S. Hullavarad, N.V. Hullavarad, P.C. Karulkar, A. Luykx, P. Valdivia, *Nanoscale Research Lett.* **2007**, 2, 161- 167.

5 Y.Hu, Y. Chang, P. Fei, R.L. Snyder, Z.L. Wang, *ACS Nano* **2010**, 4, 1234-1240.

6 Y. Liu, Z. H. Kang, Z. H. Chen, I. Shafiq, J. A. Zapien, I. Bello, W. J. Zhang, S. T. Lee., *Crystal Growth & Design* **2009**, 9, 3222- 3227.

7 X.Fan,J.Li, D.Zhao,D.Shen,B.Li, X.Wang, *J. Phys. Chem. C* **2009**, 113,21208-21212.

8 C.B.Tay, S.J.Chua, K.P. Loh, *J. Phys. Chem. C* **2010**, 114, 9981-9987.

9 L. E. Greene, M. Law, D. H. Tan, M. Montano, J. Goldberger, G. Somorjai, P.Yang, *Nano Lett.* **2005**, 5, 1231-1236.

10 D. Ehrentraut, H. Sato, Y. Kagamitani, H. Sato, A. Yoshikawa, T. Fukuda, *Prog. Cryst. Growth Charact. Mater.* **2006**, 52, 280-335.

11 Jih-Jen Wu and Sai-Chang Liu, *Adv. Mater.* **2002**, 14, 215-218.

12 Chih-Cheng Lin, Wang-Hua Lin, Chun-Yen Hsiao, Kuo-Min Lin and Yuan-Yao Li., *J. Phys. D : Appl. Phys.* **2008**, 41, 045301/1-045301/6.

13 X. Wang, J. Song, J. Liu, Z. L. Wang, *Science* **2007**, 316, 102-105.

14 P.Yang, H.Yan, S.Mao, R.Russo, J.Johnson, R.Saykallay, N. Morris, J. Phan, R. H, H.J. Choi, *Adv. Func. Mater.* **2002**, 12, 323-331.

15 G. Frens, *Nature Phys. Sci.* **1973**, 241. 20-22.

16 T. Shimada, *Thin Solid Films* **2006**, 515, 1568-1572.

17 R. H. Pierson, A. N. Fletcher, E. Sr. Clair Gantz, *Anal. Chem.* **1956**, 28, 1218-1239.

18 G. Kwak, K. Yong , *J. Phys. Chem. C.* **2008**, 112, 3036-3041.

19 D. R. Lide (ed), *CRC Handbook of Chemistry and Physics, 84th Edition*, CRC Press. Boca Raton, Florida, 2003

20 N. S. Ramgir, K. Subannajui, Y. Yang, R. Grimm,R. Michiels, M. Zacharias., *J. Phys. Chem. C.* **2010**, 114, 10323-10329.

21 R. T. Rajendra Kumar, E. McGlynn, M. Biswas, R. Saunders, G. Trolliard, B. Soulestin, J.-R. Duclere, J. P. Mosnier, and M. O. Henry, *J. Appl. Phys.* **2008**, 104, 084309/1-084309/11.

22 H.-M. Cheng, H.-C. Hsu, S. Yang, C.-Y. Wu, Y.-C. Lee, L.-J. Lin, W.-F. Hsieh, *Nanotechnology* **2005**, 16, 2882-2886.

23 D.-H. Kuo, B.-J. Chang, *Crystal Growth & Design* **2010**, 10, 977-982.

Figure captions

Fig.1 Schematic diagrams of equipment used in this research. (a) is that of TG, and (b) is that of atmospheric pressure solid source CVD.

Fig.2 TG results : time versus weight loss of ZnO. Red line is without ethanol bubbling, and blue is with ethanol bubbling.

Fig.3 Arrhenius plot calculated by TG results.

Fig.4 IR absorption spectra of exhaust gas of solid source CVD. Upper graph (a) is measured before heating source, and lower one (b) is measured during reaction.

Fig.5 SEM images of ZnO on ITO substrate. (a) is that substrate temperature is 400^{o}C, (b) is 450^{o}C, (c) is 500^{o}C, (d) is 550^{o}C, and (e) is 600^{o}C.

Fig.6 AFM image of the surface of an ITO substrate used in this experiment. The substrate temperature was 550^{o}C. RMS roughness of the surface was approximately 2.7nm and many nanoscale particles were observed.

Fig.7 SEM images of ZnO on Si substrates. (a) is that substrate temperature is 300^{o}C, (b) is 350^{o}C, (c) is 400^{o}C, (d) is 450^{o}C, and (e) is 500^{o}C. (b), (d) are rather thin film like. In narrow scale, (a),(c), and (e) has skeleton crystals but (b), (d) does not have.

Fig.8 SEM images of ZnO on Si substrate with gold NPs. (a) is top view and (b) is cross-section. The substrate temperature was 450^{o}C.

Fig.9 SEM images. (a) is gold NPs with low density on Si substrate, (b) is top view of ZnO nanorods grown in the area of gold NPs with low density, and (c) is cross-section. (d) is gold NPs with high density on Si substrate, (e) is top view of ZnO nanorods grown in the area of gold NPs with high density, and (f) is cross-section. The substrate temperature of (b),(c),(e),and (f) is 450^{o}C.

Fig.10 XPS spectra. (a) and (b) are the spectra of ZnO nanorods grown on Si substrate with gold NPs by solid source CVD method (substrate temperature was 450^{o}C). (c) is the spectrum of Si substrate with gold NPs annealed at 450^{o}C for 30min. There were no gold peaks in (a) and (b).

Fig.11 Relationship between reaction time and length of ZnO nanorods.

Table titles

Table 1 XRD peak intensity of ZnO on Si(100)

Table 2 XRD peak intensities of ZnO on three substrates grown at 450^{o}C.

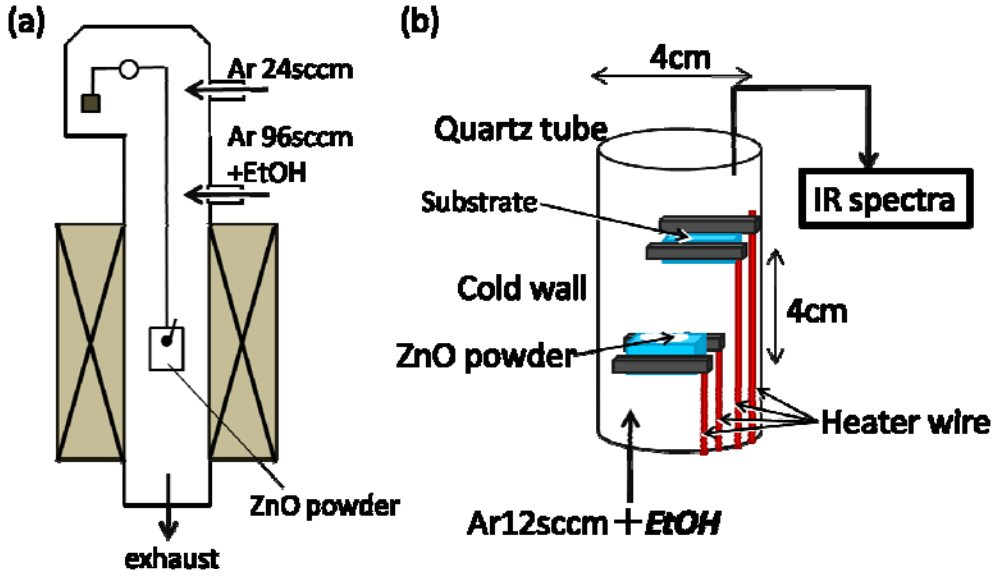

Fig.1　Schematic diagrams of equipment used in this research. (a) is that of TG, and (b) is that of atmospheric pressure solid source CVD.

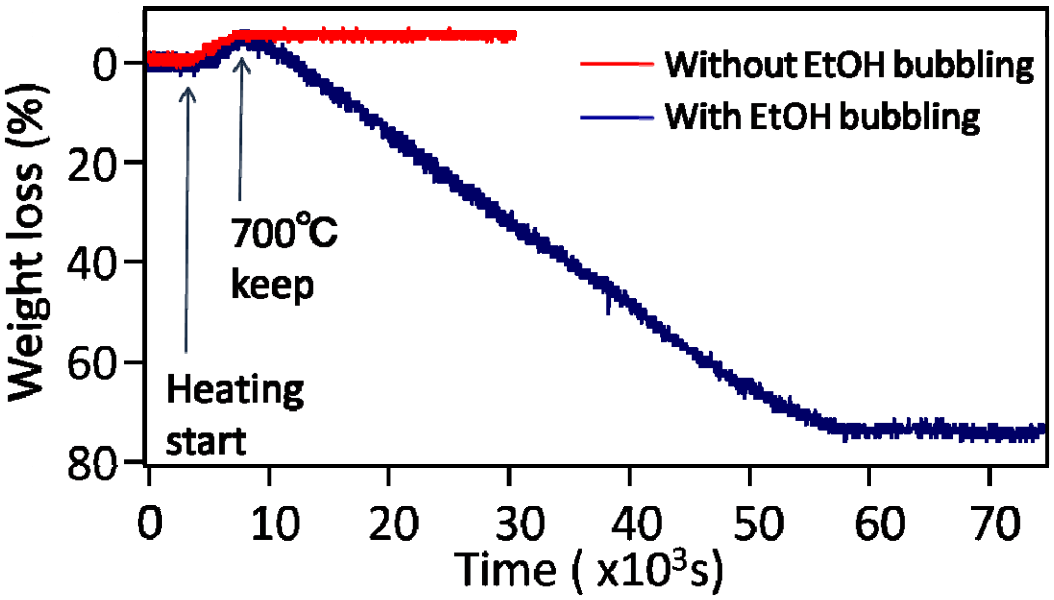

Fig.2 TG results：time versus weight loss of ZnO. Red line is the result in condition without ethanol bubbling, and blue one is the result in condition with ethanol bubbling.

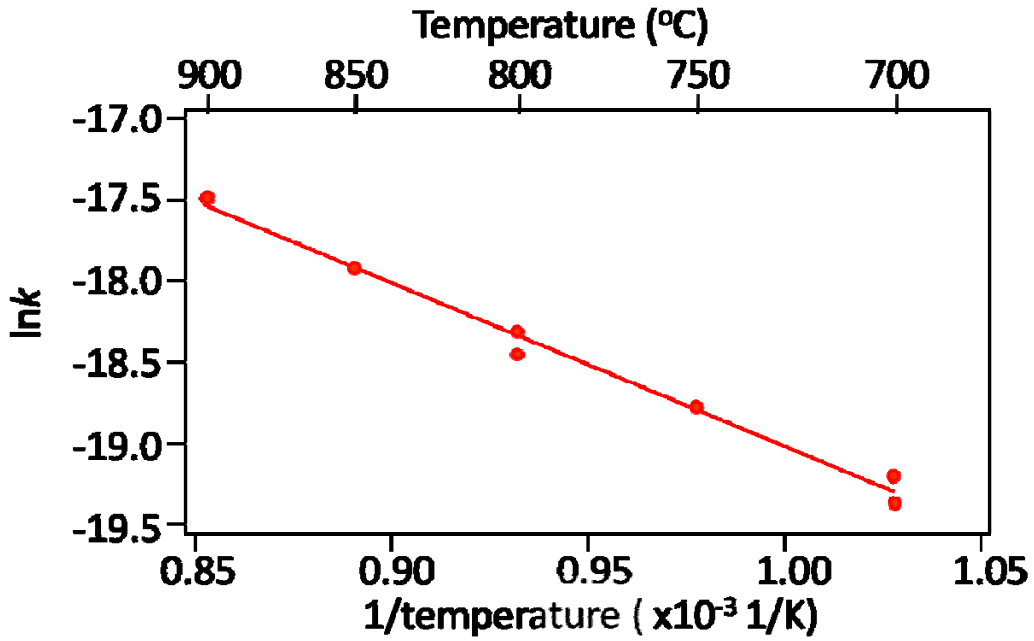

Fig.3 Arrhenius plot calculated by TG results.

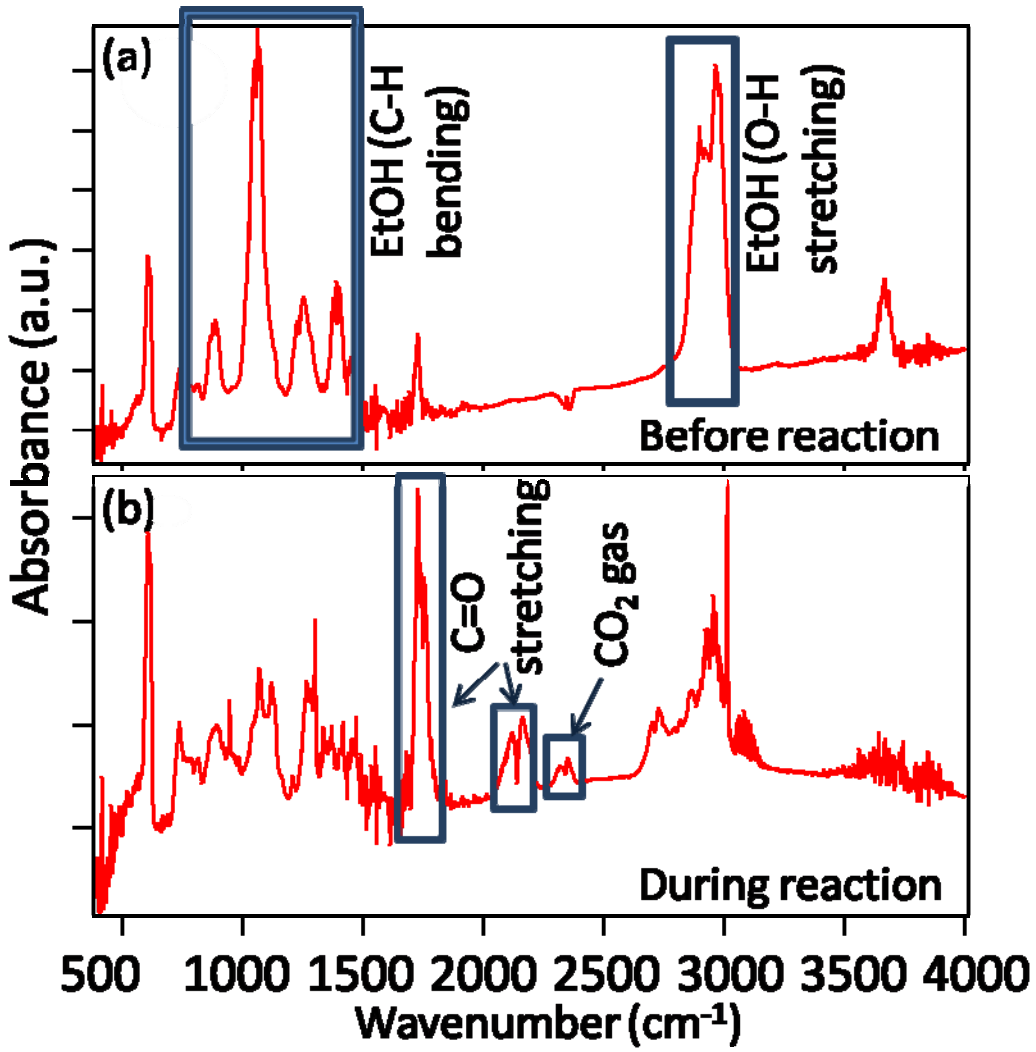

Fig.4 IR absorption spectra of exhaust gas of solid source CVD method. Upper graph (a) is measured before heating source, and lower one (b) is measured during reaction.

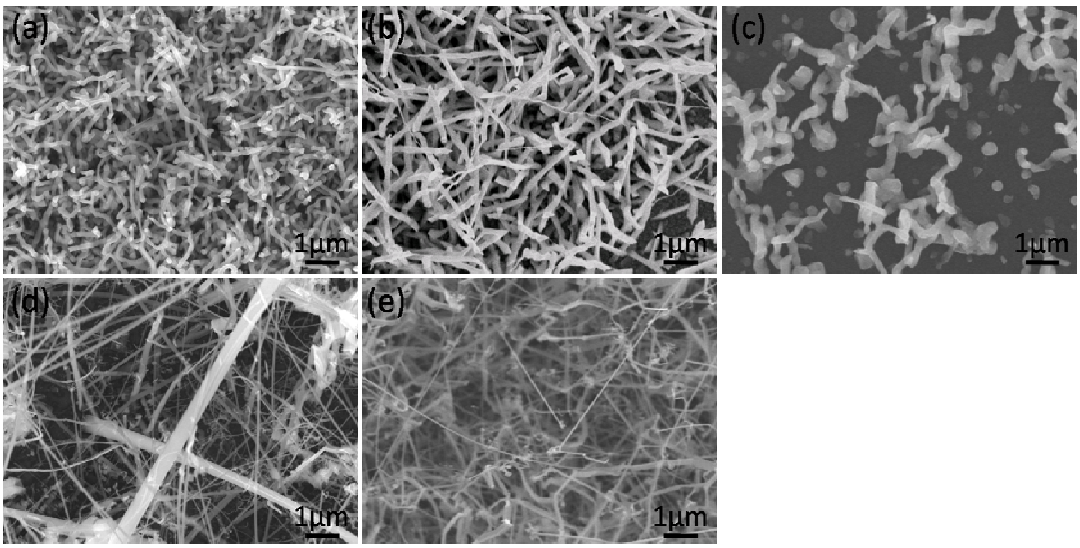

Fig.5 SEM images of ZnO on ITO substrate. (a) is that substrate temperature is 400°C, (b) is 450°C, (c) is 500°C, (d) is 550°C, and (e) is 600°C.

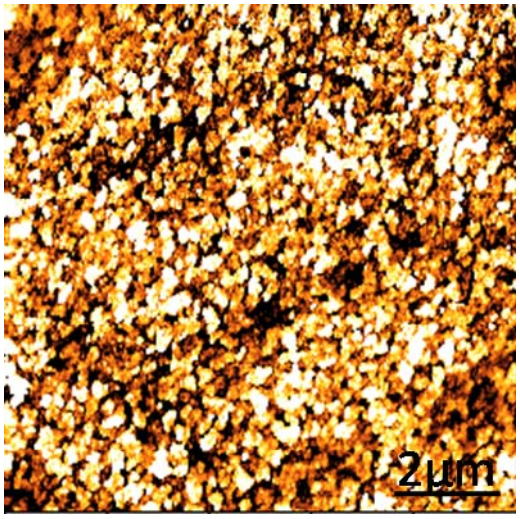

Fig.6 AFM image of the surface of an ITO substrate used in this experiment. The substrate temperature was 550°C. RMS roughness of the surface was approximately 2.7nm and many nanoscale particles were observed.

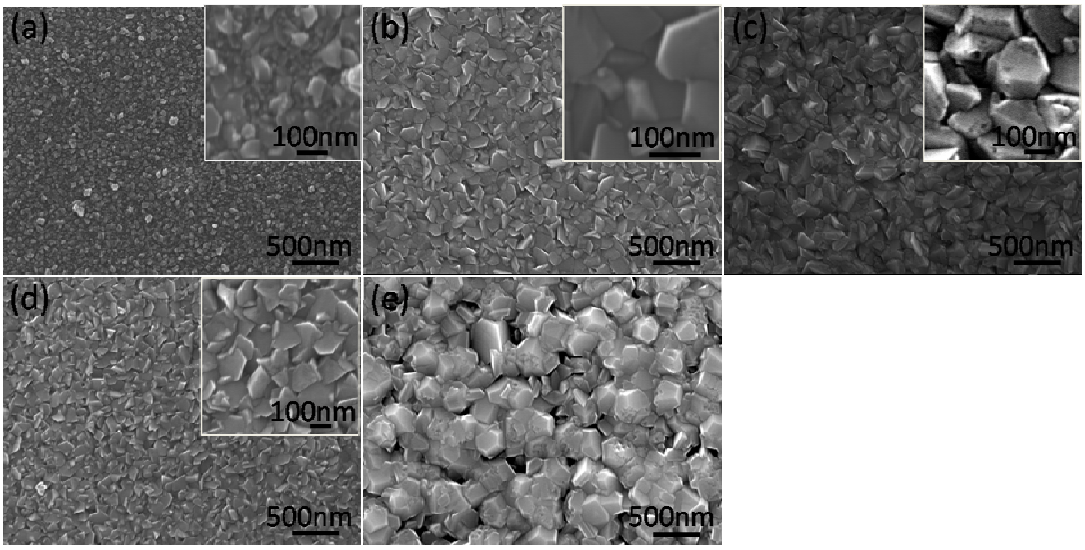

Fig.7　SEM images of ZnO on Si substrates. (a) is that substrate temperature is 300°C, (b) is 350°C, (c) is 400°C, (d) is 450°C, and (e) is 500°C. (b), (d) are rather thin film like. In narrow scale, (a),(c), and (e) has skeleton crystals but (b), (d) does not have.

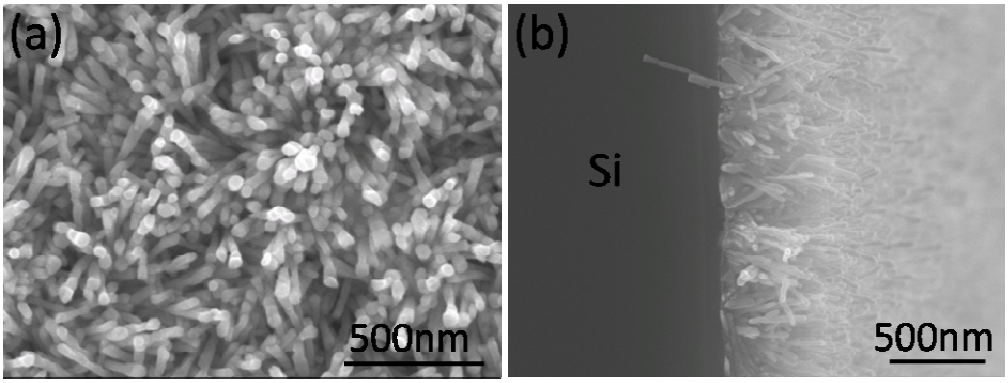

Fig.8　SEM images of ZnO on Si substrate with gold NPs. (a) is top view and (b) is cross-section. The substrate temperature was 450°C.

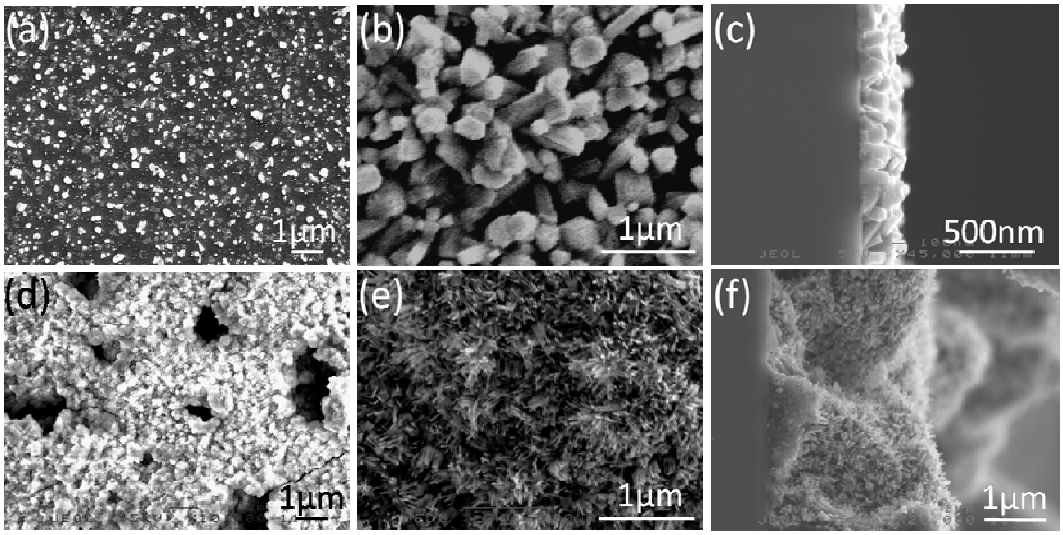

Fig.9 SEM images. (a) is gold NPs with low density on Si substrate, (b) is top view of ZnO nanorods grown in the area of gold NPs with low density, and (c) is cross-section. (d) is gold NPs with high density on Si substrate, (e) is top view of ZnO nanorods grown in the area of gold NPs with high density, and (f) is cross-section. The substrate temperature of (b),(c),(e),and (f) is 450°C.

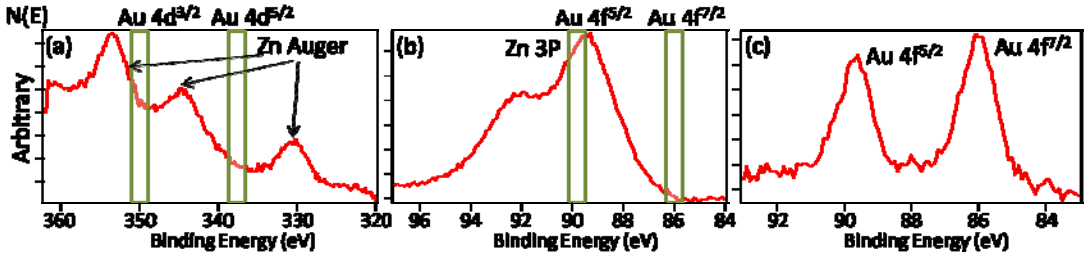

Fig.10 XPS spectra. (a) and (b) are the spectra of ZnO nanorods grown on Si substrate with gold NPs by solid source CVD method (substrate temperature was 450°C). (c) is the spectrum of Si substrate with gold NPs annealed at 450°C for 30min. There were no gold peaks in (a) and (b).

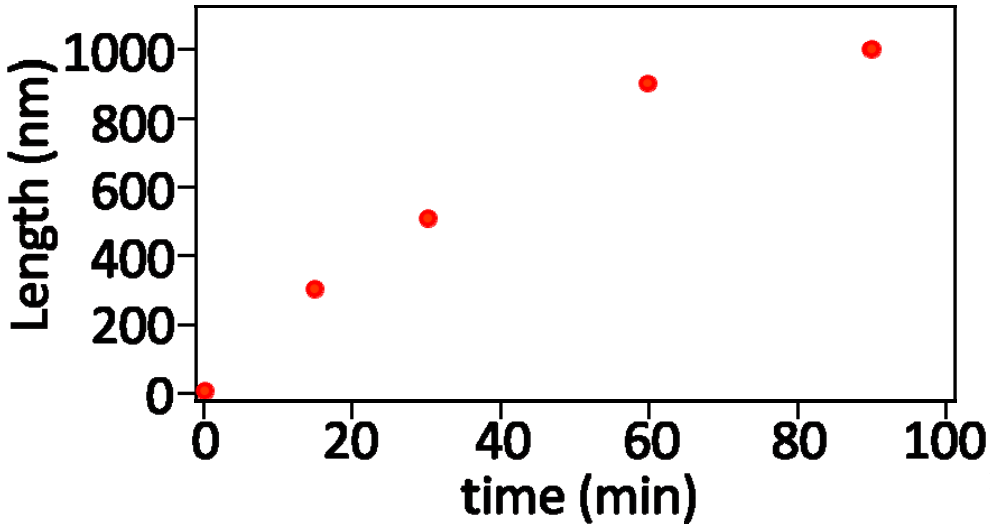

Fig.11　Relationship between reaction time and length of ZnO nanorods.

Table 1　XRD peak intensity of ZnO on Si(100)

Substrate temperature	300°C	350°C	400°C	450°C	500°C
(100):(002):(101)	2:5:5	1:13:3	2:2:3	1:12:2	1:1:2

Table 2　XRD peak intensities of ZnO on three substrates grown at 450°C.

substrate	ITO	Si(100)	Si with gold NPs
(100):(002):(101)	2:1:3	1:12:2	4:4:3

Figure for Graphical Abstract